Journal of Magnetics 12(2), 72-76 (2007)

Non-Equilibrium Green Function Method in Spin Transfer Torque

Chun-Yeol You*

Department of Physics, Inha University, Incheon 402-751, Korea

(Received 16 May 2007)

We investigate the spin transfer torque in metallic multilayer system by employing Keldysh non-equilibrium Green function method. We study the dependences of the spin transfer torque on the detailed energy configuration of ferromagnetic, spacer, and lead layers. With Keldysh non-equilibrium Green function method applied to a single band model, we explore spin transfer torque effect in various layer structures and for various material parameters.

Keywords : spin transfer torque, non-equilibrium Green function, current induced magnetization switching

1. Introduction

Spin transfer torque (STT) is one of the exciting phenomena in the recent studies of modern magnetism [1-5]. The STT is related novel spintronic devices such as current induced magnetization switching (CIMS) and domain wall motion (CIDWM). Especially, the CIMS device can overcome the selectivity and scalability problems in conventional magnetoresistance random access memory (MRAM) and pave the way to the commercialization of spin torque MRAM [6]. The CIMS due to the spin transfer torque occurs at magnetic trilayer structures with two ferromagnetic layers separated by a non-magnetic layer. And it is basically non-equilibrium phenomena since strong current flows are necessary to induce the magnetization switching. Since spin polarized current carries spin angular momentum from one ferromagnetic layer to another ferromagnetic layer, non-equilibrium physics must be employed for the proper treatment of the problem. One of the successful tools to address such a problem is the non-equilibrium Green function method developed by Keldysh [7]. Recently, Edwards *et al.* developed a self-consistent theory for CIMS by employing the Keldysh Green function method for the current perpendicular to plane (CPP) metallic multilayer geometry [8]. With in the same framework, the STT in the magnetic tunneling junction (MTJ) is also reported [9], and anomalous bias dependence of the STT is predicted [10].

*Corresponding author: Tel: +82-32-860-7667,
Fax: +82-32-872-7652, e-mail: cyyou@inha.ac.kr

In this study, we apply the Keldysh non-equilibrium Green function method for the STT [8] to various layer structures. We calculate the dependences of the STT on the energy configurations of ferromagnetic, non-magnetic spacer and lead layer, respectively. It is found that the effect of the STT can be tailored by band structure engineering such as alloying.

2. Theoretical Model

We briefly introduce the Keldysh Green function method for the STT [8]. The considered layer structure is schematically sketched in Fig. 1. The layer consists of a semi-infinite left lead layer, a finite fixed ferromagnetic layer (polarizer layer), a non-magnetic metallic spacer layer, a free ferromagnetic layer (switching layer), and a semi-infinite right lead layer as shown in Fig. 1. Each layer can be described by a tight binding model, which can describe general multi-orbit band structure. Here, we consider only single band model for simplicity. In order to handle the STT, the surface Green function method has great advantage [11-13]. With a help of surface Green function method, we can treat easily any kind of layer structure. According to Ref. [8], the spin current at n-th layer is given by $\langle j_n \rangle = \langle j_n \rangle_1 + \langle j_n \rangle_2$:

$$\langle j_n \rangle_1 = \frac{1}{4\pi} \sum_{k_\parallel} \int d\omega \mathrm{Re}[\mathrm{Tr}\{(\mathrm{B}-\mathrm{A})\vec{\sigma}\}[f(\omega-\mu_L)+f(\omega-\mu_R)]], \quad (1)$$

$$\langle j_n \rangle_2 = \frac{1}{2\pi} \sum_{k_\parallel} \int d\omega \mathrm{Re}\left[\mathrm{Tr}\left\{ \left(g_L \mathrm{TAB} g_R^\dagger \mathrm{T}^\dagger - \mathrm{AB} + \frac{1}{2}(\mathrm{A}+\mathrm{B}) \right) \vec{\sigma} \right\} \times f(\omega-\mu_L) - f(\omega-\mu_R) \right]. \quad (2)$$

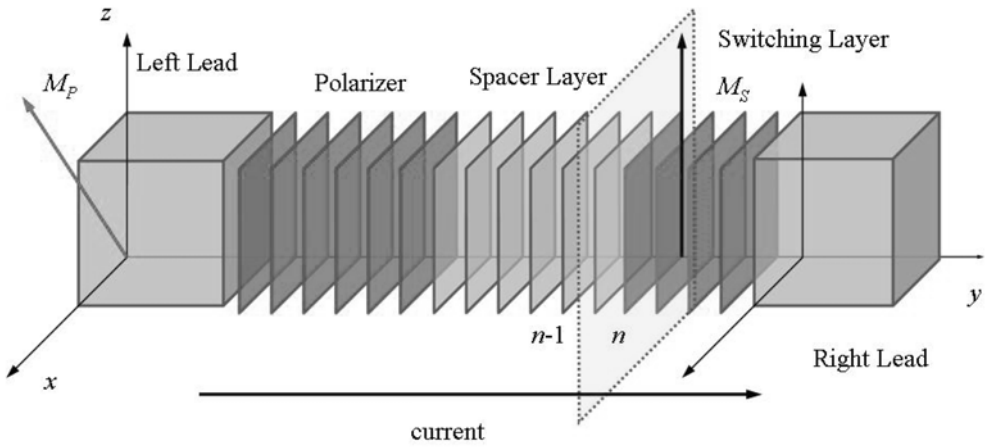

Fig. 1. Schematic sketch of the layer structure. The semi-infinite left lead layer is placed at the left side, and finite ferromagnetic layer (polarizer), *N*-atomic non-magnetic metallic spacer layer, *M*-atomic ferromagnetic layer (switching layer) are sequentially deposited. The other semi-infinite right lead layer is also placed at the right side. The direction of the magnetization of polarizer layer is placed in the *xz*-plane with angle θ from positive *z*-axis. And the switching layer magnetization direction is parallel to the positive *z*-axis.

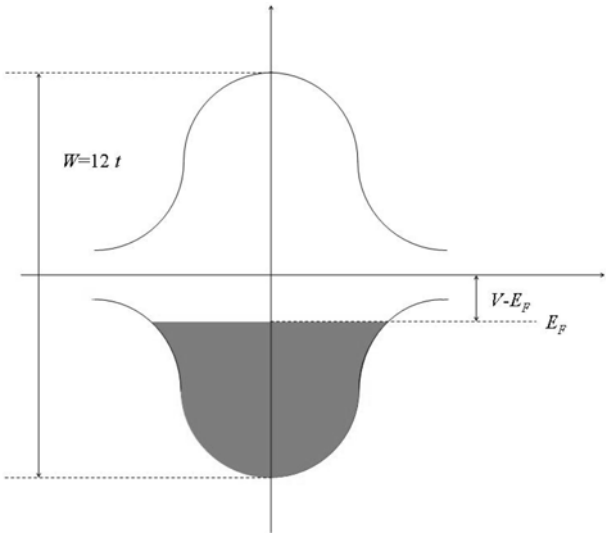

Fig. 2. Schematic diagram of the band structure of the tight binding model. The band width $W = 12t$ is depicted.

Here, $A=[1-g_R T^{\dagger} g_R T]^{-1}$, $B=[1-g_R^{\dagger} T^{\dagger} g_R^{\dagger} T]^{-1}$ and $f(\omega-\mu)$ is the Fermi distribution function with chemical potential μ. μ_L and μ_R are the chemical potential of left and right leads such that $\mu_L - \mu_R = eV_b$, bias voltage. $\vec{\sigma}$ is the Pauli matrix vector, and T is a hopping matrix. g_L are g_R the surface Green functions for the decoupled equilibrium system, and they are 2×2 matrices for the single band model. The decoupled equilibrium surface Green functions can be evaluated in a straightforward way for a given band structure. More details can be found in Ref. [8] and references therein. In this study the nearest neighbor hopping parameter $t = 0.5$ eV and the band width $W = 12t = 6$ eV is taken for the whole system as shown in Fig. 2.

The physical meaning of $\langle j_n \rangle_1$ and $\langle j_n \rangle_2$ are already clearly explained in [8], Recalling that $\langle j_n \rangle_1$ is related with the interlayer exchange coupling [13] and the interlayer exchange coupling decays as square of the spacer layer thickness, $\langle j_n \rangle_1$ may be neglected for thick non-magnetic spacer layer cases.

3. Results and Discussions

In Fig. 3, we plot the $T_{\perp,1}=\langle j_{Spacer}\rangle_1-\langle j_{Lead}\rangle_1$ as a

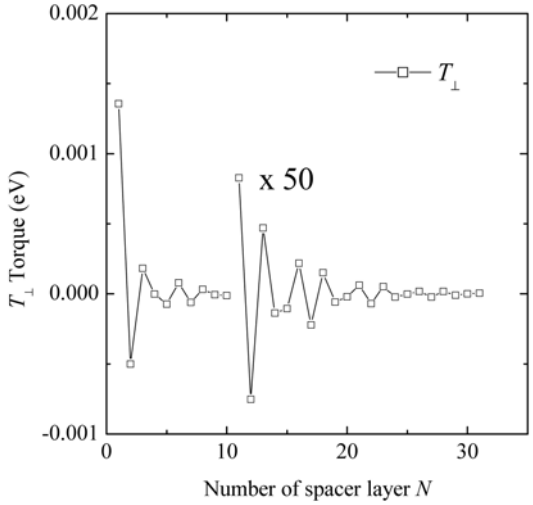

Fig. 3. $T_{\perp,1}=\langle j_{Spacer}\rangle_1-\langle j_{Lead}\rangle_1$ as a function of the non-magnetic spacer layer thickness *N*. With increasing N, it decreases while exhibiting an oscillation. The data ($N > 10$) are magnified by 50 times.

Table 1. Band energy configurations. $V_{P,S}^{\uparrow,\downarrow}$ are on-site potentials for spin up and down for polarizer and switching layer, and V_{Spacer} is for the spacer layer, respectively. N, M_p and M_s are the number of atomic layer for the spacer, polarizer and switching layers. Each energy has a unit of eV.

case	$V_P^{\uparrow}$	$V_P^{\downarrow}$	V_{Spacer}	$V_S^{\uparrow}$	$V_S^{\downarrow}$	V_{Lead}	N	M_p	M_s
(A)	2.3	3.0	2.3	2.3	3.0	2.3	1-30	∞	5
(B)	2.3	3.0	2.3	2.3	3.0	2.3	20	∞	5
(C)	2.3	3.0	2.0-3.0	2.3	3.0	2.3	20	∞	5
(D)	2.3	3.0	2.3	2.3	3.0	2.0-3.0	20	∞	5
(E)	2.3	3.0	2.3	2.3	2.3-3.4	2.3	20	∞	5

function of the non-magnetic spacer layer thickness. Here $\langle j_{Spacer}\rangle_1$ and $\langle j_{Lead}\rangle_1$ are $\langle j_n\rangle_1$ terms at the rightmost layer of the spacer and the leftmost layer of the right lead, respectively. We take the parameters of case (A) in Table 1 for this calculation. It is clearly shown that $T_{\perp,1}$ term decreases with oscillation, which is a well-known property of the oscillatory interlayer exchange coupling in a trilayer structure [14].

From now on, we will consider only $\langle j_n\rangle_2$ term, which is related to the torque, T, exerting at the switching layer as follows [8]:

$$T=\langle j_{Spacer}\rangle_2-\langle j_{Lead}\rangle_2 . \quad (3)$$

The in-plane, $T_\parallel = T_x$, and out-of-plane, $T_\perp = T_x$, components are plotted as a function of the angle θ between magnetization directions of polarizer and switching layers in Fig. 4. The case (B) in Table I is considered in this calculation. The spacer layer thickness N is fixed to 20, and we set $V_P^{\uparrow} = V_S^{\uparrow} = V_{Spacer} = V_{Lead}$. This case mimics the Co/Cu/Co system since the band structure of Cu is well matched with fcc Co majority one. This result is the reproduction of Ref. [8]. $T_{\perp,1}$ is depicted together for the

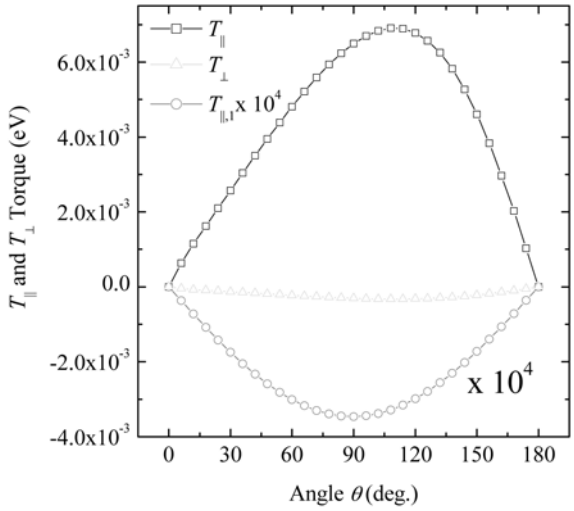

Fig. 4. In-plane, $T_\parallel$, and out-of-plane, $T_\perp$, components are plotted as a function of the angle θ between the magnetization directions of the polarizer and switching layers. The unit of torque $T_\parallel$ is eV_b. For the comparison, $T_{\perp,1}\times 10^4$ is also shown.

comparison. As aforementioned the interlayer exchange coupling, $T_{\perp,1}$, term is much smaller than the spin torque term for $N = 20$. The angular dependence of STT is almost $\sin\theta$ even though there exist small deviations.

We vary the on-site energy of the spacer layer V_{Spacer} and V_{Lead} lead layer from 2.0 to 3.0 eV for the case (C) in Table 1. Figure 5 shows the schematic energy configurations and Fig. 6(a) and (b) show the results. When V_{Spacer} varies from 2.0 to 3.0 eV, $T_\parallel$ have its maximum for $V_{Spacer} \sim V_S^{\uparrow} = V_P^{\uparrow}$, as shown in Fig. 6(a). The V_{Lead} variation shows very similar behavior wtih, $V_{Lead} \sim V_S^{\uparrow} = V_P^{\uparrow}$, resulting in maximum $T_\parallel$. It is clear that $T_\parallel$ is a function of the energy band structure of not only spacer layer, but also the lead layer. It is worthwhile to note that $V_{Cu} \sim V_{Co}^{\uparrow}$,

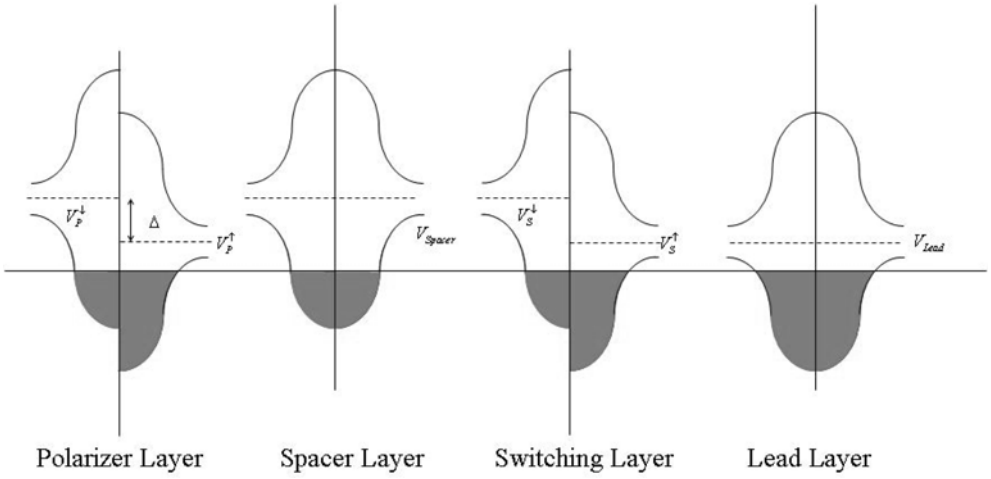

Fig. 5. Variation of the on-site energy of the spacer layer, V_{Spacer}, and lead layer, V_{Lead}. The results of Fig. 6 (a) are calculated with fixed V_{Lead} and varying V_{Spacer}, and the results of Fig. 6(b) are calculated with fixed V_{Spacer} and varying V_{Lead}.

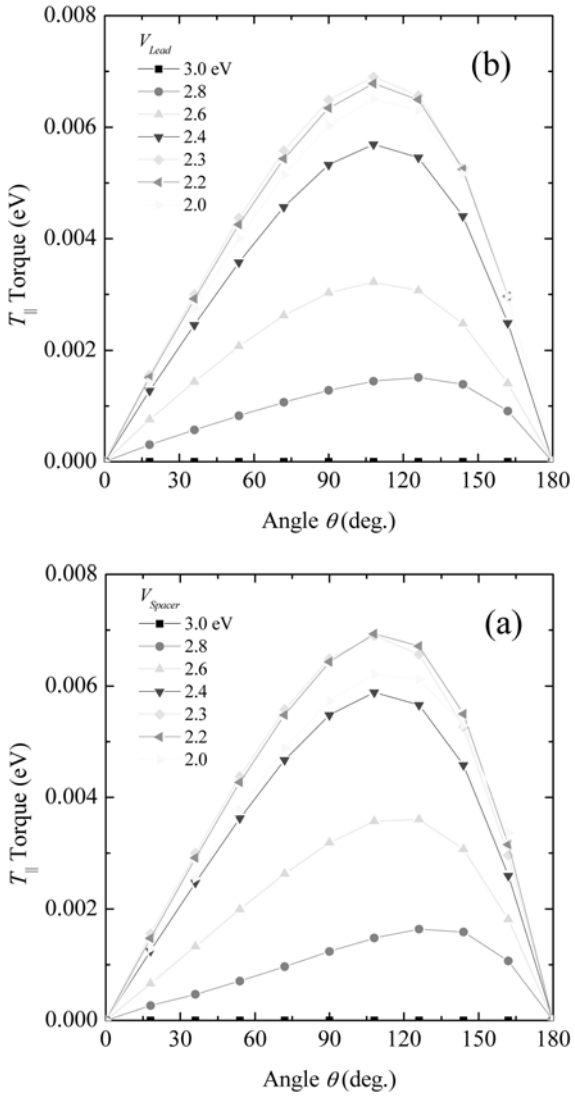

Fig. 6. $T_\parallel$ and $T_\perp$ for (a) various V_{Spacer}(case (C) in Table I), (b) various V_{Lead} (case (D) in Table 1).

while $V_{\mathrm{Ru}} \sim V_{\mathrm{Co}}^{\downarrow}$. Therefore Co/Cu/Co/Cu is near the best combinations, and Co/Ru/Co/Cu is near the worst combination.

Next, we vary the exchange splitting energy of the switching ferromagnetic layer, $\Delta = V_S^{\downarrow} - V_S^{\uparrow}$ while that for the polarizer layer is fixed, case (E). Figure 7 shows the STT as a function of Δ for $\theta=\pi/2$. The results indicate that large exchange splitting energy generates strong STT, but it saturates for $\Delta \sim 0.7$ eV. It is surprising that the STT is not a monotonic increasing function of Δ. Instead it oscillates as depicted in Fig. 7. $T_\parallel$ and $T_\perp$ show their peak values at $\Delta \sim 0.35$ and 0.15 eV, respectively. The physical origin of the unexpected oscillation is not clear, however, it may be ascribed to a resonance due to the wave nature of the electron spins.

It must be noticed that the Keldysh non-equilibrium

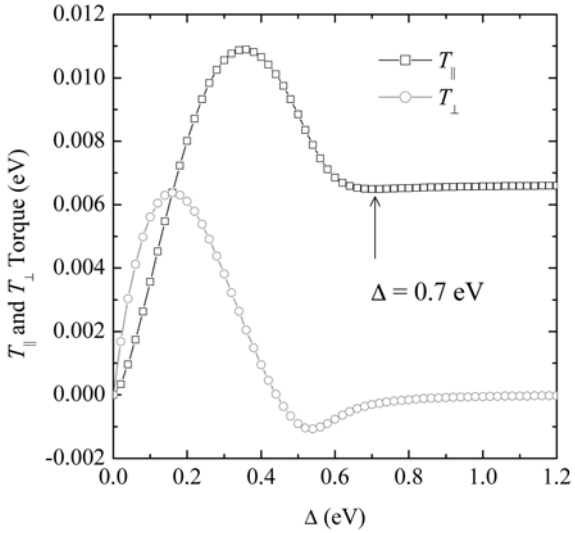

Fig. 7. $T_\parallel$ and $T_\perp$ as a function of Δ, case (E) in Table 1.

Green function formalism presented in this paper is optimized for the ballistic transport, and it does not include the effect of diffusion. In metallic system, the spin accumulation due to the diffusion is important [15]. In this study, such spin accumulation is not taken into account.

4. Conclusions

We study the spin transfer torque in metallic multilayer system with the Keldysh non-equilibrium Green function method. The band structure dependent STT is calculated for various cases. We find that the STT effect can be enhanced with proper design of the band configurations of the ferromagnetic, non-magnetic spacer, and lead layers.

Acknowledgement

This work was supported by the Korea Research Foundation Grant funded by the Korean Government (MOEHRD) (KRF-2005-070-C00053) and CYY thanks to Prof. J. Mathon and K.-J. Lee for the helpful discussions.

References

[1] J. C. Slonczewski, J. Magn. Magn. Mater. **159**, L1 (1996): L. Berger, Phys. Rev. B **54**, 9353 (1996).

[2] E. B. Myers, D. C. Ralph, J. A. Katine, R. N. Louie, and R. A. Buhrman, Science **285**, 867 (1999): S. I. Kiselev, J. C. Sankey, I. N. Krivorotov, N. C. Emley, R. J. Schoelkopf, R. A. Buhrman, and D. C. Ralph, Nature **425**, 380

(2003).
[3] Y. Tserkovnyak, A. Brataas, G. E. W. Bauer, and B. I. Halperin, Rev. of Mod. Phys. **77**, 1375 (2005).
[4] A. Brataas, G. E. W. Bauer, and P. J. Kelly, Phys. Rep. **427**, 157 (2006).
[5] J. C. Lee, M. G. Chun, W. H. Park, C.-Y. You, S.-B. Choe, W. Y. Yung, and K. Y. Kim, J. Appl. Phys. **99**, 08G517 (2006).
[6] M. Hosomi *et al.*, Electron Devices Meeting, 2005. IEDM Technical Digest, IEEE International, 459 (2005).
[7] L. V. Keldysh, Sov. Phys. JETP **20**, 1018 (1965).
[8] D. M. Edwards, F. Federici, J. Mathon, and A. Umerski, Phys. Rev. B. **71**, 054407 (2005).
[9] A. Kalitsov, I. Theodonis, N. Kioussis, M. Chshiev, W. H. Butler, and A. Vedyayev, J. Appl. Phys. **99**, 08G501 (2006).
[10] I. Theodonis, N. Kioussis, A. Kalitsov, M. Chshiev, and W. H. Butler, Phys. Rev. Lett. **97**, 237205 (2006).
[11] J. Mathon, Phys. Rev. B. **56**, 11810 (1997).
[12] J. Mathon, A. Umerski, and Murielle Villeret, Phys. Rev. B. **55**, 14378 (1997).
[13] J. Mathon, Murielle Villeret, A. Umerski, R. B. Muniz, J. d'Albuquerque e Castro, and D. M. Edwards, Phys. Rev. B. **56**, 11797 (1997).
[14] M. D. Stiles, J. Magn. Magn. Mater. **200**, 322 (1999).
[15] M .D. Stiles and A. Zangwill, Phys. Rev. B. **66**, 014407 (2002).